ANALYTICAL SCIENCES DECEMBER 2010, VOL. 26

Quantification of Polycyclic Aromatic Hydrocarbons in Water: a Comparative Study Based on Three-dimensional Excitation-emission Matrix Fluorescence

Huanbo WANG,† Yujun ZHANG, and Xue XIAO

Key Laboratory of Environmental Optics and Tecnology, Anhui Institute of Optics and Fine Mechanics, Chinese Academy of Sciences, P. O. Box 1125, Hefei 230031, Anhui, P. R. China

Excitation-emission matrix fluorescence (EEM) was proposed to quantify three polycyclic aromatic hydrocarbons of anthracene (AN), phenanthrene (PHE) and pyrene (PY) in this paper. Direct analysis through selecting the appropriate areas from the data of EEMs and another approach using all data of EEM combined with the Parallel Factor (PARAFAC) were discussed respectively. The results showed that the predicted concentrations of PHE and PY approached the actual one for both methodologies, and that the room-mean-square errors of the prediction were no more than 0.5 μg L^{-1}. In addition, a new quantificational method was suggested, in which the sum intensity around the peak value replaced the maximum intensity in the selected regions. The sensitivity can be improved ten times compared with the conventional analysis.

(Received July 4, 2010; Accepted September 24, 2010; Published December 10, 2010)

Polycyclic aromatic hydrocarbons (PAHs) are an important class of pollutants because they can be easily found in the environment, and have been identified as mutagens in bacterial and human cell assays, some of which have even been considered to be human carcinogens.[1-3] PAHs are generally formed during the incomplete combustion or pyrolysis of organic matter occurring in a variety of natural processes or human activities. The latter case is prevailing, and of greater concern. They are mainly produced during the incomplete combustion of carbon-containing materials, such as wood, coal, agricultural wastes and the operation of both diesel and gasoline engines. These pollutants can enter water through many ways, including petroleum spills, runoff from roads, sewage, effluents from industrial processes, fallout from the atmosphere and many other ways. Since PAHs are persistent, ubiquitous and toxic, sixteen of them are included in the list of priority pollutants by US Environmental Protection Agency (EPA).

Chromatography techniques are widely used for the detection and quantification of PAHs, such as gas chromatography (GC) with a flame ionization detector (FID) or mass spectrometry (MS),[4-6] high-performance liquid chromatography (HPLC) with a UV-Vis diode array detector (DAD) or fluorescence detector.[7-10] The methods mentioned above were also recommended by EPA as standard methods for the determination of PAHs.[11] For example, method 8310 provides HPLC for the detection of μg L^{-1} levels of certain PAHs, and compounds in the effluent are detected by ultraviolet and fluorescence detectors. Method 8100 provides GC with FID for the detection of certain PAHs. Since the GC procedure does not adequately resolve all 16 of the PAHs listed in priority pollutants, method 610 is restricted to use for both GC and HPLC systems to quantify these PAHs. Chromatographic analysis is highly selective, and has a low detection limit for many pollutants. Unfortunately, all of them inherently suffer from the main disadvantages associated with the need for large amounts of hazardous organic solvents as well as large sample volumes or tedious and time-consuming pretreatments.

As an alternative, fluorescence methods are proposed for the direct detection of PAHs in aqueous environment, since it is simple, sensitive, rapid and nondestructive. Conventional fluorescence spectroscopy involves generating an emission spectrum by scanning the emission wavelength (λ_{em}), while the sample is irradiated at a fixed excitation wavelength (λ_{ex}); also, an excitation spectrum is obtained by scanning the excitation wavelength while recording the emission signal at a given wavelength. Another possibility is to scan both monochromators simultaneously, which is called synchronous fluorescence spectroscopy (SFS). If the scan rate is constant for both monochromators when a constant wavelength interval is kept between λ_{ex} and λ_{em}, the technique is known as constant-wavelength SFS. The applications of these conventional fluorescence spectra methods have been described by Rodríguez in detail.[12] The traditional methods are simple and rapid, but they are featureless, and usually can not quantify multiple compounds because of their overlapping spectra. Therefore, several authors have recently described the use of excitation-emission fluorescence matrix spectra (EEM) for identifying and quantifying PAHs in water samples.[13-16] In the case of an EEM, the fluorescence intensity is collected as a function of both the excitation and emission wavelengths. Due to the additional coordinate, the data obtained by EEM is larger than that in conventional fluorescence spectra. As a result, many characteristics can be observed, and it is possible to use the EEM data to analyze the multiple PAHs directly.

Moreover, based on "mathematical separation" as a replacement of "physical or chemical separation", a great variety of chemometric algorithms, such as parallel factor analysis (PARAFAC),[17-19] alternating trilinear decomposition (ATLD),[20,21] multivariate calibration resolution (MCR)[22,23] and selfweighted

† To whom correspondence should be addressed.
E-mail: hbwang@aiofm.ac.cn

alternating trilinear decomposition (SWATLD) *etc*.,[24] have been proposed and increasingly utilized for the processing of three-way data. For example, Bosco had carried out three-dimensional excitation-emission matrix fluorescence and PARAFAC to simultaneously analyze the photodegradation process of PAHs.[25] Nie had also achieved the simultaneous determination of 6-methylcoumarin, 7-methoxycoumarin and testosterone propionate in cosmetics with EEM analysis combined with both PARAFAC and SWATLD.[26,27] Fang *et al.* quantified three fluoroquinolone antibiotics in plasma by using EEM coupled with the ATLD and PARAFAC algorithm.[28] The determination of PAHs by excitation-emission matrix fluorescence coupled with chemometric algorithms can also be found in some papers.[29–31] In this paper, two methods were proposed to quantify the PAH mixtures containing anthracene, phenanthrene and pyrene based on excitation-emission matrix fluorescence. One approach was to apply excitation-emission matrix fluorescence combined with the PARAFAC algorithm to resolve the overlapping spectra, and then to calculate the concentrations in test samples. The other one was a direct analysis using the data obtained by excitation-emission fluorescence only, in which it was analyzed according to the characteristic area of each component. Furthermore, we also discussed the sensitivity of the quantitative method using single-point (SIN) with the maximum intensity and the area integral (INT) around the fluorescence peak to regress against the concentration.

Theory

EEM fluorescence

The EEM fluorescence spectra can be obtained by collecting the emission spectra at various excitation wavelengths, and all the emission spectra compose a resultant **I** by **J** matrix, in which each of **I** row and **J** column denote the emission spectra at the *i*th excitation wavelength and the excitation spectra at the *j*th emission wavelength, respectively. The EEMs follow the tri-linear model, which can be described by

$$x_{ijk} = \sum_{n=1}^{N} a_{in} b_{jn} c_{kn} + e_{ijk}, \quad (1)$$

where x_{ijk} is the fluorescence intensity of sample k at the excitation wavelength i and the emission wavelength j; a_{in} is an element of the excitation spectra of N species; similarly, b_{jn} is an element of the emission spectra of N species, and c_{kn} is the element of the concentration matrix of N species in the k sample; e_{ijk} is the residual error.

PARAFAC algorithm

The PARAFAC algorithm[32] attacked the problem of solving qualitative and quantitative data simultaneously. Stacking a series of sample concentration matrices can make up a data cube **X**; the algorithm decomposes the cube **X** into three loading matrices (**A**, **B** and **C**), where **A**, **B** and **C** correspond to the excitation spectra, emission spectra and concentration profiles, respectively.

To find the solution in the tri-linear model, alternating least squares (ALS)[33] are employed by beginning with an initial estimate of the excitation spectra (**A**) and emission spectra (**B**) profiles, and then to estimate the concentration loadings (**C**). The algorithm proceeds to iterate until the convergence is reached.

In the calibration step, these concentration loadings (**C**) resolved by PARAFAC are regressed against the real concentration of each PAH in the mixture to obtain a calibration line. Then, the calibration line can be used to predict the concentration of each PAH in the test samples.

Table 1 Concentration of PAHs in the calibration and test set

Sample	PHE/ μg L^{-1}	PY/ μg L^{-1}	AN/ μg L^{-1}	Sample	PHE/ μg L^{-1}	PY/ μg L^{-1}	AN/ μg L^{-1}
1	0	10.0	5.0	10	1.0	10.0	6.5
2	1.0	8.0	4.0	11	2.5	8.5	3.5
3	2.0	6.0	6.0	12	4.0	7.0	5.0
4	3.0	5.0	3.0	13	5.0	6.0	2.5
5	4.0	4.0	7.0	14	6.0	5.0	8.0
6	5.0	3.0	2.0	15	7.0	4.0	1.0
7	6.0	2.0	8.0	16	8.5	2.5	10.0
8	8.0	1.0	0	17	10.0	1.0	9.0
9	10.0	0	10.0				

Core consistency diagnostic test

The traditional PARAFAC is sensitive to the number of component, N. If N is less than the number of real components, the errors associated with the PARAFAC model will be large; as a result, the estimated excitation and emission profiles will not conform to reality; if N is greater than the number of real components, it will be forced to describe minor sources of systematic instrumental errors, which will cause the estimated excitation and emission profiles not to be physically meaningful. Hence, the core consistency diagnostic (CORCONDIA) test[34] was used to determine the number of components in the present work, which can be described as follows:

$$\text{CORCONDIA} = 100 \times \left[1 - \frac{\sum_{d=1}^{N}\sum_{e=1}^{N}\sum_{f=1}^{N} (g_{def} - t_{def})^2}{\sum_{d=1}^{N}\sum_{e=1}^{N}\sum_{f=1}^{N} t_{def}^{\,2}} \right]. \quad (2)$$

In Eq. (2), g_{def} and t_{def} represent the elements of the calculated core and the super-diagonal core, respectively, and N is the number of components in the mixture. When the value is lower than 60%, the model will not satisfy the tri-linear model, and a number whose value of CORCONDIA is greater than 60% is what we need.

Figures of merit

The root-mean-squared error of the prediction (RMSEP) is calculated according to

$$\text{RMSEP} = \sqrt{\frac{\sum_{i=1}^{N} (\hat{c}_i - c_i)^2}{N}}. \quad (3)$$

The relative error of the prediction is calculated according to

$$\text{REP} = \frac{|\hat{c}_i - c_i|}{c_i} \times 100\%, \quad (4)$$

where N is the total number of components used in the model; $\hat{c}_i$ is the predicted concentration of the analyst in the ith unknown sample, and c_i is the actual concentration in the ith.

The sensitivity (SEN) can be defined as follows:

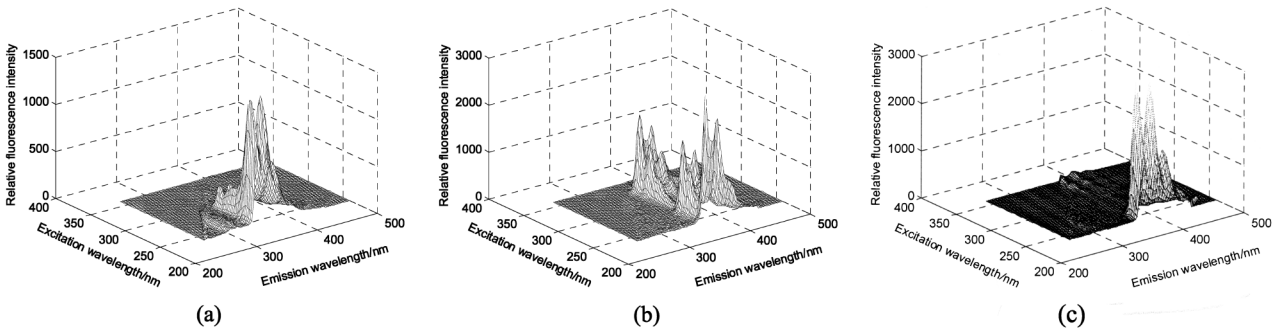

Fig. 1 Three-dimensional fluorescence plots of PHE (a), PY (b) and AN (c).

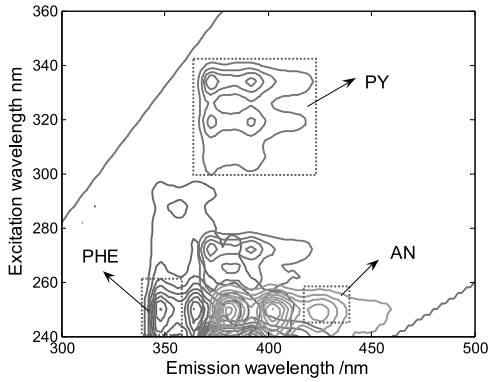

Fig. 2 Contour plot of PHE, PY and AN.

Table 2 Regression linear curve and relative coefficients for each PAH with different methods

		Regression curve	*R*
PHE	SIN	$Y = 121.6052X + 102.4821$	0.9995
	INT	$Y = 1027.8491X + 770.5479$	0.9996
	PARAFAC	$Y = 1102.3053X + 1773.3237$	0.9958
PY	SIN	$Y = 180.6280X - 4.4179$	0.9998
	INT	$Y = 1357.6955X + 54.1341$	0.9998
	PARAFAC	$Y = 2168.5736X - 29.08382$	0.9992
AN	SIN	$Y = 118.7096X + 61.7095$	0.9922
	INT	$Y = 1013.0023X + 632.7439$	0.9957
	PARAFAC	$Y = 2227.9214X + 520.4338$	0.9932

$$\mathrm{SEN} = \frac{\mathrm{d}x}{\mathrm{d}c} \tag{5}$$

SEN is the ratio between the changes in the fluorescence intensity and the concentration, which can also be considered to be the slope of the calibration line in the present work.

Experimental

Apparatus

An F-7000 fluorescence spectrophotometer equipped with a 150 W xenon lamp was used in the present work, and all measurements were performed with a 10-mm quartz cell. Operations were carried out on a personal computer under the windows XP operating systems, and the data were saved automatically.

Reagents and solutions

All of the PAHs, anthracene (AN), phenanthrene (PHE) and pyrene (PY), were purchased from Aldrich, and these reagents were used without any purification. Stock solutions (100 mg L^{-1} for each of the PAHs) were prepared by dissolving appropriate PAHs in HPLC-grade ethanol, and then the solutions were stored in a dark flask at 4°C for use. The standard solutions (100 μg L^{-1}) were made by diluting the stock solutions in deionized water, and stored under the same condition as the stock solutions. The deionozed water used was purified in a Millipore MilliQ system. The working solutions were prepared daily for use.

Analytical methods

To determine these PAHs, a set of 17 samples were prepared in terms of their linear analytical range of AN, PHE and PY. The first nine samples with the concentration in the range 0 – 10 μg L^{-1} for each PAH were used as a calibration set; the following eight samples were designed as a test set with the concentration corresponding to the calibration set. The concentrations in each sample are listed in Table 1.

The EEMs were recorded at excitation wavelengths from 240 to 360 nm, and emission wavelengths from 260 to 500 nm with a 2-nm interval, making a total of 6161 data points for each sample; both the excitation and emission slits were set at 5 nm. The measurements were performed at 700 V with a scanning rate of 12000 nm min^{-1}.

Due to the presence of the Rayleigh scattering in the range of the wavelengths we choose, which may have an effect on the analysis, we set the values above the Rayleigh scattering line to zero so as to reduce the influence; in addition, Raman scattering could be minimized by subtracting the deionozed water blank for each sample.

Results and Discussion

Analysis of single EEM

Figure 1 shows three-dimensional excitation-emission fluorescence plots of pure AN, PHE and PY. The Rayleigh and Raman scattering lines have been truncated from the image. As shown in Fig. 1, PHE exhibited three peak regions, in which $\lambda_{ex}/\lambda_{em}$ are at 250/348, 250/364 and 250/384 nm, respectively; there was more than one peak region in the plot of PY; λ_{em} are around 372 and 392 nm, λ_{ex} are distributed very widely, and the peak areas can all be found at 240, 272, 320 and 334 nm.

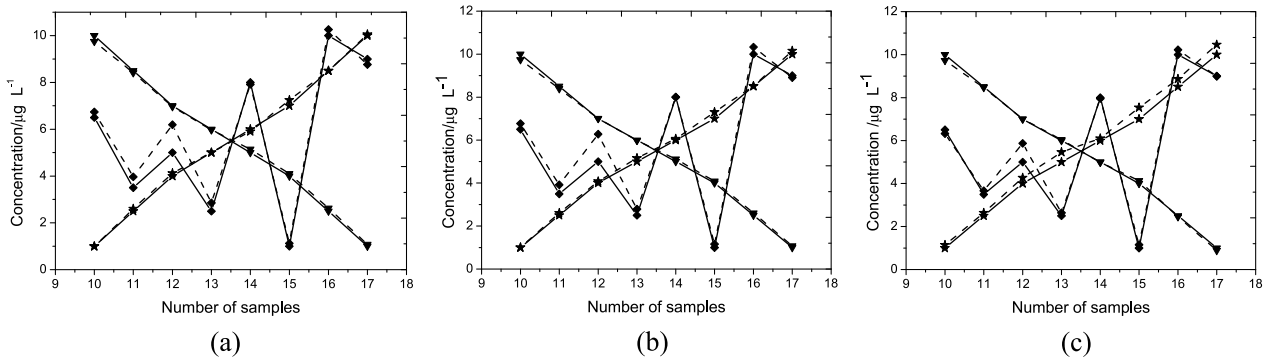

Fig. 3 Predicted and actual concentrations *versus* the number of samples by different methods: SIN (a), INT (b) and PARAFAC (c); dash line represents the calculated concentration and solid line represents the actual concentration; triangle, diamond and five-point star are denoted by PY, AN and PHE, respectively.

Table 3 Relative errors for each PAH obtained by different methods

Sample	PHE, %			PY, %			AN, %		
	SIN	INT	PARAFAC	SIN	INT	PARAFAC	SIN	INT	PARAFAC
10	0.59	0.13	13.61	2.50	2.64	2.77	3.68	4.16	27.11
11	4.03	4.21	5.23	0.99	1.32	0.36	13.33	11.91	4.64
12	3.05	1.92	6.67	0.49	0.06	0.04	23.78	25.61	17.38
13	0.14	3.17	9.31	0.43	0.29	0.71	13.96	11.56	5.49
14	1.63	0.94	1.74	2.97	2.34	0.22	1.04	0.03	0.53
15	3.53	4.27	7.63	2.57	2.08	3.47	11.97	16.15	15.48
16	0.03	0.19	4.36	5.03	4.14	1.88	2.58	3.26	2.22
17	0.51	1.55	4.64	8.01	7.49	11.59	2.58	1.01	0.06

For AN, the peak regions appeared at the excitation wavelength near 250 nm and the emission wavelength at approximately 380, 402 and 424 nm, respectively. Each PAH had a specific fluorescence peak area; and these fluorescence characteristics can be used for both qualitative and quantitative analysis.

Synthetic sample calibration and quantification

The data in an EEM can also be visually presented in the form of a fluorescence contour plot that can separate different components of a multi-component system into isolated peaks. The contour plot of a single component for AN, PHE and PY is shown in Fig. 2. The spectra overlap very seriously within the regions when the excitation wavelengths were from 240 to 280 nm, and the emission wavelengths were between 375 and 410 nm. Therefore, choosing appropriate fluorescence peak regions used to quantifying these mixtures was crucial; not only should it contain more fluorescence information of each analyst, but should also avoid any overlapping areas. Considering all of the conditions, we selected the rectangle regions, identified by dotted lines, to quantify the mixtures.

Initially, SIN analysis using the maximum intensity *versus* the concentration was performed in the selected areas, where the excitation/emission wavelength pairs ($\lambda_{ex}/\lambda_{em}$) corresponding to the maximum intensity were at 250/348, 334/372 and 250/424 nm for PHE, PY and AN, respectively. The maximum intensities were regressed against the concentration of each PAH in the mixture to obtain a calibration curve. Table 2 gives these regression lines; the regression coefficients (R) are higher than 0.99 in all cases. Furthermore, the predicted concentrations in the test samples are presented in Fig. 3. As shown in Fig. 3(a), the predicted concentrations of PHE and PY were consistent with the actual ones, whereas AN had an evident deviation from the real concentration in the test samples of numbers 11 and 12, which may have been caused by the overlapping spectra of PY. The relative errors are summarized in Table 3. The relative errors are no more than 15% for both PHE and PY, but are slightly larger for AN; the maximum error achieved to was 27%.

In fact, SIN analysis as a traditional method has been utilized by most authors. However, the maximum intensity may not always appear at a fixed excitation/emission wavelength for an analyst at different concentrations, it may show a slight shift sometimes. An efficient method using the total fluorescence intensity around the maximum intensity replaced the maximum intensity to regress against the concentration was proposed in the present work.

The method of the INT can be described as follows: first, finding out the maximum intensity in the selected regions, and then choosing an integral region to calculate the sum of the fluorescence intensity; finally, regressing the sum of the fluorescence intensity *versus* the concentration. Different integration regions had been selected to examine the performance of the new method, which is presented in Fig. 4(a), and an enlarged figure of PHE is shown in Fig. 4(b). The integration regions of AN and PY were similar to PHE. Analytical results using different integration region are given in Table 4. It was clearly demonstrated that the sensitivity obtained by the INT method improved by nearly 10 times compared with the SIN measurement, since the single-to-noise greatly increased. However, when enlarging the integration region, the selectivity become worse because the coefficient was smaller, especially

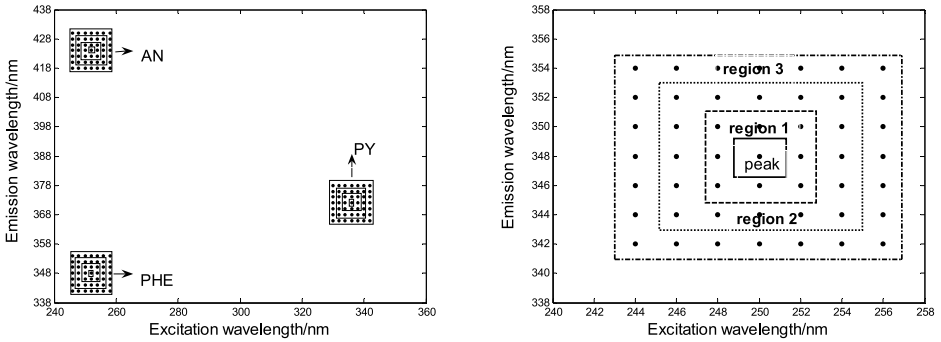

(a) (b)

Fig. 4 Different integration regions for AN, PHE and PY (a) and the enlarged figure of PHE (b).

Table 4 The analytical results of AN, PHE and PY by INT method choosing different integration region

Integration region	PHE			PY			AN		
	Grid data	SEN	*R*	Grid data	SEN	*R*	Grid data	SEN	*R*
Peak point	1 × 1	121.6	0.9995	1 × 1	180.6	0.9998	1 × 1	118.7	0.9922
Region 1	3 × 3	1027.8	0.9996	3 × 3	1357.6	0.9998	3 × 3	1013.0	0.9957
Region 2	5 × 5	2620.9	0.9943	5 × 5	2852.9	0.9996	5 × 5	2474.9	0.9906
Region 3	7 × 7	4128.9	0.9977	7 × 7	4185.6	0.9991	7 × 7	4174.9	0.9865

Table 5 Statistical parameter and figures of merit for each PAH obtained by different methods

	PHE			PY			AN		
	SIN	INT	PARAFAC	SIN	INT	PARAFAC	SIN	INT	PARAFAC
RMSEP	0.1110	0.1409	0.3487	0.1257	0.1224	0.1184	0.4941	0.5138	0.3366
REP	1.6887	2.0475	6.6487	2.8737	2.545	2.63	9.115	9.2112	9.1137
SEN	121.6	1027.8	1102.3	180.6	1357.6	2168.5	118.7	1013.0	2227.9

for AN, which changed from 0.9957 to 0.9865. At the same time, the sensitivity become less because the characteristic variation of the region far from the peak position was not significant. Thus, a square area with nine data points, including the peak value as its center, was the best integration region, in which the sensitivity was higher and the selectivity was not lost. In conclusion, three ways should be considered before choosing the integral region: first, the characteristic variation of spectral intensity should be significant; second, do not include the scatter regions; finally, the overlapped region should be avoided.

The regression equations and the predicted concentration are given in Table 2 and Fig. 3, respectively. The results are similar to that obtained by the SIN method. The figures of merit are listed in Table 5, the RMSEPs were less than 0.2 μg L^{-1} for PHE and PY, and the value was slightly higher for AN, which is up to 0.5 μg L^{-1}.

Quantification of PAHs using PARAFAC algorithm

In practical cases, the samples of our interest also consist of some interference, and the PARAFAC algorithm is sensitive to the factors, so the number of components should be designated in advance. In the present work, a CORCONDIA test was used to estimate the optimal number, and one to five factors were chosen to calculate the core consistency. The results are given in Table 6. As can be appreciated, two factors gave a core consistency value equal to 100%, and the value of three factors was 98.8%. However, when using four or more factors, the values lead to a great decrease. The results indicated that three factors were appropriate for applying the PARAFAC algorithm, which is in accord with the fact.

Table 6 Core consistency values for PARAFAC models using one to five factors

Number of factors	1	2	3	4	5
CORCONDIA, %	100	100	98.8	20.61	0

Excitation and emission spectra resolved by PARAFAC are shown in Fig. 5. The predicted concentration calculated by PARAFAC algorithm is shown in Fig. 3(c). As shown in Fig. 3, the result was more poor than that of both methods mentioned above for PHE, whereas the concentration of AN was more satisfactory. The figures of merit, including RMSEP, REP and SEN, are listed in Table 5. From Table 5 we can conclude that a good performance had been achieved to quantify the mixtures of PHE, PY and AN by the PARAFAC. However, the PARAFAC algorithm took a much longer time than the direct analysis procedure for the calculations.

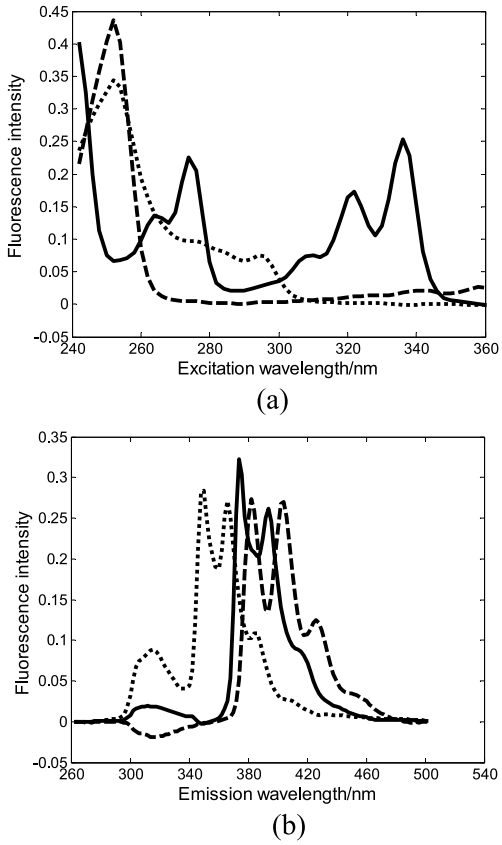

Fig. 5 Excitation spectra (a) and emission spectra (b) resolved by PARAFAC algorithm; the dashed, solid and dotted line represent AN, PY and PHE, respectively.

Conclusions

Excitation-emission matrix fluorescence provided an alternative method to the characterization and quantification of PAHs. EEMs coupled with the PARAFAC algorithm was performed to predict the concentrations of PHE, PY and AN in this paper. The results showed that RMSEPs were no more than 0.5 μg L^{-1} for each of the PAHs, and the sensitivity was also higher than any other procedures. At the same time, a direct analysis method was also discussed. Similar results of figures of merit can be obtained using SIN and INT method, except for the sensitivity. The sensitivity was increased by 10 times with the INT method than the SIN method.

Acknowledgements

This project was supported by Hi-Tech Research and Development Program of China (No. 2007AA061502) and the Natural Science Foundation of AnHui (090415215).

References

1. M. S. Flint, B. L. Hood, M. Sun, N. A. Stewart, J. Jones-Laughner, and T. P. Conrads, *J. Proteome Res*., **2010**, *9*, 509.
2. K. Kuhn, B. Nowak, G. Klein, A. Behnke, A. Seidel, and A. Lampen, *J. Food Protect*., **2008**, *71*, 993.
3. E. Papa, P. Pilutti, and P. Gramatica, *Sar Qsar Environ. Res*., **2008**, *19*, 115.
4. J. J. Langenfeld, S. B. Hawthorne, and D. J. Miller, *Anal. Chem*., **1996**, *68*, 144.
5. L. Xu and H. K. Lee, *J. Chromatogr., A*, **2008**, *1192*, 203.
6. R. Ong, S. Lundstedt, P. Haglund, and P. Marriott, *J. Chromatogr., A*, **2003**, *1019*, 221.
7. S. Danyi, F. Brose, C. Brasseur, Y. J. Schneider, Y. Larondelle, L. Pussemier, J. Robbens, S. De Saeger, G. Maghuin-Rogister, and M. L. Scippo, *Anal. Chim. Acta*, **2009**, *633*, 293.
8. I. Windal, L. Boxus, and V. Hanot, *J. Chromatogr., A*, **2008**, *1212*, 16.
9. M. Bourdat-Deschamps, J. J. Daudin, and E. Barriuso, *J. Chromatogr., A*, **2007**, *1167*, 143.
10. F. Portet-Koltalo, K. Oukebdane, L. Robin, F. Dionnet, and P. L. Desbene, *Talanta*, **2007**, *71*, 1825.
11. R. D. JiJi, G. A. Cooper, and K. S. Booksh, *Anal. Chim. Acta*, **1999**, *397*, 61.
12. J. J. S. Rodríguez and C. P. Sanz, *Lumin. Spectrosc*., **2000**, *28*, 710.
13. M. L. Nahorniak and K. S. Booksh, *Analyst*, **2006**, *131*, 1308.
14. Y. C. Kim, J. A. Jordan, M. L. Nahorniak, and K. S. Booksh, *Anal. Chem*., **2005**, *77*, 7679.
15. M. V. Bosco, M. P. Callao, and M. S. Larrechi, *Anal. Chim. Acta*, **2006**, *576*, 184.
16. M. L. Nahorniak and K. S. Booksh, *J. Chemom*., **2003**, *17*, 608.
17. O. Divya and A. K. Mishra, *Appl. Spectrosc*., **2008**, *62*, 753.
18. A. Muñoz de la Peña, A. Espinosa Mansilla, N. Mora Díez, D. Bohoyo Gil, A. C. Olivieri, and G. M. Escandar, *Appl. Spectrosc*., **2006**, *60*, 330.
19. J. H. Christensen, G. Tomasi, J. Strand, and O. Andersen, *Environ. Sci. Technol*., **2009**, *43*, 4439.
20. X. M. Wang, H. L. Wu, J. F. Nie, Y. N. Li, Y. J. Yu, and R. Q. Yu, *Sci. China, Ser. B: Chem*, **2008**, *51*, 729.
21. Y. Zhang, H. L. Wu, A. L. Xia, S. H. Zhu, Q. J. Han, and R. Q. Yu, *Anal. Bioanal. Chem*., **2006**, *386*, 1741.
22. M. C. G. Antunes and J. C. G. Esteves da Silva, *Anal. Chim. Acta*, **2005**, *546*, 52.
23. A. Espinosa-Mansilla, A. Muñoz de la Peña, H. C. Goicoechea, and A. C. Olivieri, *Appl. Spectrosc*., **2004**, *58*, 83.
24. H. Deng and L. P. Shang, *Spectrosc. Spect. Anal*., **2009**, *29*, 1088.
25. M. V. Bosco and M. S. Larrechi, *Talanta*, **2007**, *71*, 1703.
26. J.-F. Nie, H.-L. Wu, S.-H. Zhu, Q.-J. Han, H.-Y. Fu, S.-F. Li, and R.-Q. Yu, *Talanta*, **2008**, *75*, 1260.
27. J.-F. Nie, H. Wu, X. Wang, Y. Zhang, S. Zhu, and R. Yu, *Anal. Chim. Acta*, **2008**, *628*, 24.
28. D.-M. Fang, H.-L. Wu, Y.-J. Ding, L.-Q. Hu, A. L. Xia, and R.-Q. Yu, *Talanta*, **2006**, *70*, 58.
29. J. A. Arancibia and G. M. Escandar, *Anal. Chim. Acta*, **2007**, *584*, 287.
30. S. A. Bortolato, J. A. Arancibia, and G. M. Escandar, *Anal. Chem*., **2008**, *80*, 8276.
31. A. A. Eiroa, E. V. Blanco, P. L. Mahia, S. M. Lorenzo, and D. P. Rodriguez, *Analyst*, **1998**, *123*, 2113.
32. R. A. Harshman, *UCLA Working Papers in Phonetics*, **1970**, *16*, 1.
33. F. Yates, *The Empire Journal of Experimental Agriculture*, **1933**, *1*, 129.
34. R. Bro and H. A. L. Kiers, *J. Chemom*., **2003**, *17*, 274.